Cement & Concrete Composites 34 (2012) 166–171

Contents lists available at SciVerse ScienceDirect

Cement & Concrete Composites

journal homepage: www.elsevier.com/locate/cemconcomp

Tensile and bending behaviour of a strain hardening cement-based composite: Experimental and numerical analysis

Jean-Louis Tailhan, Pierre Rossi *, Claude Boulay

Institut Français des Sciences et Technologies des Transports, de l'Aménagement et des Réseaux (IFSTTAR, previously L.C.P.C.), Université Paris-Est, France

ARTICLE INFO

Article history:
Received 9 December 2010
Received in revised form 11 October 2011
Accepted 15 October 2011
Available online 20 October 2011

Keywords:
Ultra-high performances cement-based composite
Bending behaviour
Uniaxial tensile behaviour
Numerical modelling
Inverse analysis

ABSTRACT

IFSTTAR has developed a Multi-Scale Cement Based Composite (MSCC). This composite material is strain hardening in tension and exhibits ultra-high strengths as well in both compression and tension. The main research objectives for the present paper are the determination of the strain hardening properties of the material: using a newly developed tensile test in conjunction with a finite-element-based inverse analysis, the input parameters of an (adapted) numerical model can be identified. Therefore, numerical simulations can be performed to describe the bending behaviour of a thin slab having a thickness representative of the corresponding industrial application.

The main conclusions of this study are:

- The studied material clearly exhibits strain hardening in tension with a uniaxial tensile strength of about 20 MPa and a modulus of rupture of about 50 MPa.
- Elasto-plastic behaviour with strain hardening is a relevant mechanical model (for the studied material) for designing (by the finite element method) structural elements behaving principally in bending.

1. Introduction

Based on the "multi-scale fibre reinforcement" concept proposed by Rossi et al. [1], a Multi-Scale Cement Based Composite (MSCC) has been developed and patented [2–8]. This cement based composite is obtained by incorporating a high percentage of steel fibres in an ultra-high performance matrix (with a compressive strength of more than 250 MPa). This fibre reinforcement is composed of three different geometries (different lengths and diameters) of fibres, each one playing a particular role in relation with the matrix cracking process at a corresponding scale. By this way, a real strain hardening material is expected. The steel fibre reinforcement of this MSCC (the total volume percentage being equal to 11% by volume of concrete) can be summarised as follows:

- *First dimension:* steel wool with a fibre length less than 2 mm (between 1% and 3%).
- *Second dimension:* straight drawn fibre 5 mm long and 0.15 mm in diameter (between 4% and 6%).
- *Third dimension:* straight drawn fibre 20 mm long and 0.25 mm in diameter (between 1% and 3%).

Further details regarding the material composition and its processing are reported elsewhere [2–8].

Taking into account the *cost/performance* ratio for this kind of material, it is necessary to optimise its industrial use. In 2-D thin structures (e.g. plates, thin slabs or shells) when they are principally subjected to bending or to point loads, the material is essentially in a local tensile state of stress. As a consequence, to design a plate (or a thin slab) with a finite element model, it is important to know, and then to determine, the tensile behaviour of the material.

The principal objective of this study is to demonstrate that a mechanical model taking into account "classical" elasto-plastic behaviour with strain hardening is pertinent to design structures made with the studied material. To achieve this objective, the following steps are chosen:

- First, a uniaxial tensile test is developed and performed to verify that the studied material is really a strain hardening one. This type of test is not easy to perform correctly on this kind of material (as discussed in Chapter 2).

* Corresponding author. Address: LCPC-58, Boulevard Lefebvre – 75732 Paris Cedex 15, France. Tel.: +33 1 40 43 52 95; fax: +33 1 40 43 54 93.
E-mail address: pierre.rossi@lcpc.fr (P. Rossi).

0958-9465/$ - see front matter © 2011 Elsevier Ltd. All rights reserved.
doi:10.1016/j.cemconcomp.2011.10.005

– Secondly, bending tests are performed on specimens representative of industrial structural elements considered as pertinent applications with the studied material.
– Third, a finite element model is used to simulate the experimental bending tests. The values of the model parameters are determined by a semi-inverse analysis.
– Lastly, possible scale effect problems related to the values of the model parameters are analysed.

During this study, only the pre-peak behaviour is considered for both experimental and modelling aspects (in both bending and uniaxial tension). This means that the material softening behaviour is not considered and analysed in this work. The reason is that only the strain hardening behaviour of the material is retained to design structures made of the studied material. This design strategy seems to be suitable when 2-D thin structures are considered.

2. Uniaxial tensile test development

It is interesting to note that some researchers have worked on the development of uniaxial tensile tests adapted to study ultra-high performance cement-based composites [9,10]. In the present study, the objective of this tensile test is to determine the uniaxial tensile behaviour of the studied MSCC when it is used in a thin slab element (or plate). So, the fibre distribution must be representative of the one which exists within a thin slab or a plate, i.e. it must be orthotropic. Therefore, it has been decided that the width of the specimen, in the uniform tensile zone, has to be at least four times larger than the length of the largest fibre: a length of 10 cm seems relevant.

Other criteria also intervened in the definition of the specimen geometry:

- Strain and stress fields in the specimen zone where strain measurements are carried out should be as uniform as possible, and over a sufficient length with respect to the length of the largest fibre: a measurement base of 20 cm is therefore selected.
- Specimen must not crack in the zone located close to the interface between the specimen and the test/machine grip. In this zone, the strain and the stress fields are not uniform.
- Previous studies [9] on cement composites, with a matrix similar to that of the studied material, indicated that this matrix starts to crack for a tensile stress of about 8 MPa. In comparison with these previous studies, the uniaxial tensile strength of the studied MSCC can reach 25 MPa, i.e. approximately three times the tensile strength of its matrix.

According to the criteria and above remarks, the specimen dimensions have to respect the following conditions: 5 cm thickness, 10 cm width, and 20 cm length, in the zone where strain and stress fields must be as uniform as possible. Moreover, the specimen must have a 30 cm width at the interface level with the press (so that stress is approximately three times lower than that of the zone where strain measurements are carried out).

Taking the works of Do [11] and Behloul [12,13] as a starting point, a dog bone specimen with 75 cm of overall length is retained at this step of the study. The specimen, glued to the press by using an adaptation block (made of aluminium), has its geometry (and dimensions) optimised by numerical simulations using the CESAR-LCPC finite element code. This optimisation aims to:

– generate uniform tensile stress in the central part of the dog bone specimen;
– generate much lower tensile stresses (compared to the central part of the specimen) at the *specimen/press* interfaces.

Taking into account the specimen shape and in the aim to avoid tensile stress appearance as consequence of material restrained shrinkage during its stay in mould after casting, particular cares, following those mentioned by Behloul [13], are taken. The moulds are manufactured to be able to run nine specimens in three batches. Specimen and mould geometries are given in Fig. 1. Specimens are cast flat and are vibrated during casting on a mobile plate. All specimens have undergone a heat treatment (in a drying oven at 90 °C for 4 days, 48 h after their removal from mould).

After this cure, the upper and lower faces of each specimen are ground with a surface grinder machine. Twenty minutes before the tests, the specimens are glued, with a methyl methacrylate resin, between two platens, made of aluminium alloy, rigidly fixed on the cross-heads of the testing machine.

To ensure that no crack appears in glued interfaces during the test, it has been decided to add complementary supports placed on specimen concave parts. These supports are connected to the specimen and to the aluminium platens via four 20 mm diameter prestressed rods (Fig. 2). In order to design them, finite element calculations, still using the CESAR-LCPC code, were performed taking into account all experimental set-ups (that means with the prestressing of the interface zone between the specimen and the machine). The calculations showed that tensile stresses at *specimen/press* interfaces reached 8.5 MPa when it reached 27 MPa in specimen central part (where the stress distribution was found to be homogeneous).

Four specimens are tested following the experimental set-up described above. A jack displacement rate of 0.1 mm/min is imposed.

3. Bending tests

In this study, prefabricated thin slab element (or plate) is considered as a structural application of the MSCC. Mechanical tests are thus carried out on specimens representative of these types of structural elements. In order to optimise specimens dimensions with respect to scale effects and to preferential orientation of fibres, it is selected to retain the following dimensions for the specimens: 600 mm length, 200 mm width and 40 mm thickness.

The specimens are cast flat and vibrated during casting on a mobile plate. *Specimen width/largest fibre length* ratio (200/25) and specimen casting procedure allow an orthotropic orientation of fibres representative of a real slab element. A four point bending test

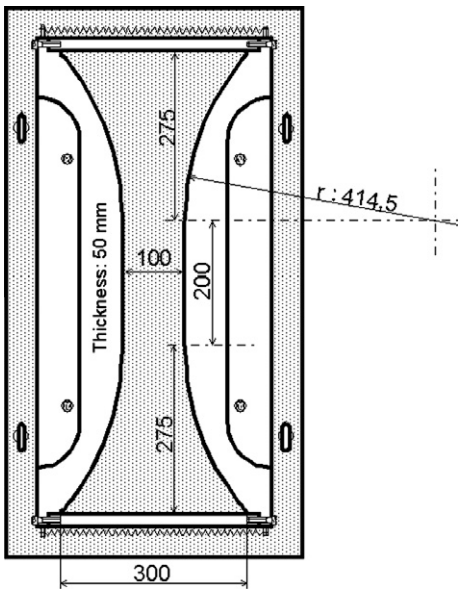

Fig. 1. Specimen mould and geometry related to the tensile test.

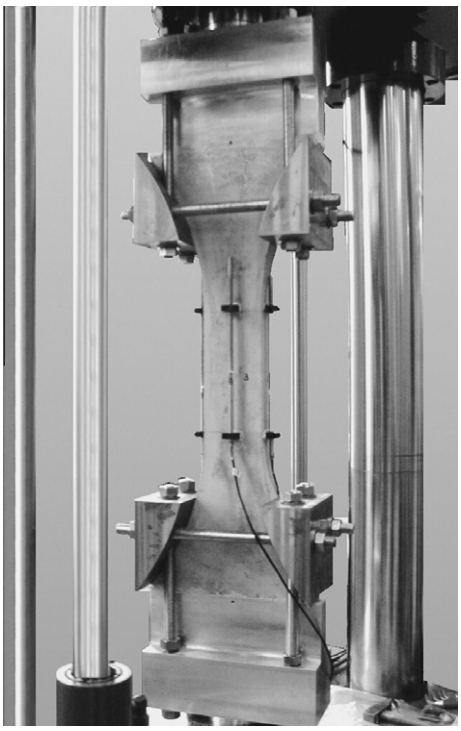

Fig. 2. Uniaxial tensile test set-up.

is performed. The distance between the lower supports is 420 mm; and between the upper supports is 140 mm.

Tests were carried out at an imposed deflection rate equal to 0.3 mm/min. Deflection is measured using an extensometer placed on the specimens to eliminate parasitic displacements at the level of the supports. Nine specimens have undergone a heat treatment similar to that of the tensile specimens and six specimens have undergone a cure with water.

4. Experimental results

4.1. Uniaxial tensile tests

Strain measurements are realised by using four transducers (LVDT) glued on each specimen face in its central part on a base length of 200 mm (Fig. 2). Fig. 3 presents strain–stress curves given by the four transducers. It is a representative example of responses of the four specimens tested.

This Fig. 3 shows that the values given by the four transducers are similar up to the maximum load. Therefore, we can consider strain in the specimen central part as being homogeneous. So, it is relevant to determine the specimen tensile strain by considering the average value of the four displacements.

This result is important. As a matter of fact, it is very difficult, with a strain hardening cement-based composite containing such a high percentage of fibres, to avoid a non-negligible bending of the specimen during the tensile loading. Then, a specimen bending can cause a spurious strain hardening. The previous works found in literature (evocated before) have not clearly discussed and treated this aspect.

Fig. 4 gives four *strain–stress* curves obtained with the four tested specimens. Only pre-peak stress behaviour is considered (as explained before). It confirms that the material is strain hardening in tension.

Fig. 5 presents an example crack pattern at the end of the test (in the softening behaviour part of the test). It shows the existence of multi-macrocracking. However, it is important to note that, for all specimens, any visible cracks were detected until the peak load. (The eye is able to detect an opening crack around 50 μm.)

4.2. Bending tests

Results are given in Fig. 6. An average modulus of rupture of about 50 MPa is observed. (The modulus of rupture is calculated by using Eq. (1), given in Section 6, which is the classical formula of the strength of materials theory.)

The material seems to remain elastic up to a limit near to 45% of the maximum load. The material becomes interesting when its hardening behaviour (from 45% to 100% of the maximum load) is considered. At the maximum load, the maximum strain measured (using a displacement transducer of length 140 mm) on the specimen lower face is 5×10^{-3}. In this range of loading, visible cracks were not detected. Moreover, two strain gauges of length 70 mm are glued on the lower face of one specimen, over a length of measurement of 140 mm. No crack localisation is detected before approximately 60% of the maximum load, and after this point, in spite of the ***weak*** and regular divergence of measurements between the two gauges (the damage in the constant moment zone is no more totally homogeneous), material regularly continues to be entirely loaded up to the peak neighbourhood. At the peak load a visible crack finally appears which signals crack localisation.

5. Numerical modelling

Taking into account all experimental observations and results described above concerning, firstly, the material global mechanical responses (in tension and in bending) and, secondly, the diffuse character of cracking mechanisms before maximum loads, material is supposed to follow an elastic–plastic behaviour with hardening up to its maximum carrying capacity. This hypothesis does not take into account an eventual loss of rigidity of the material during its

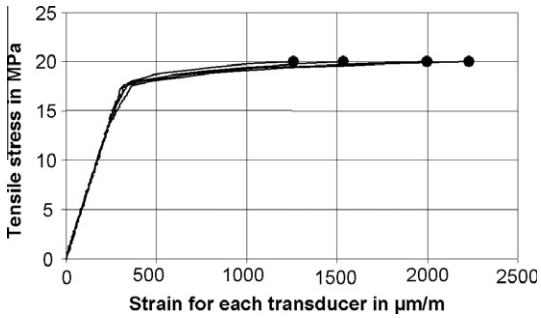

Fig. 3. Stress–strain curves given by the four transducers – example related to one of the four specimens tested in uniaxial tension.

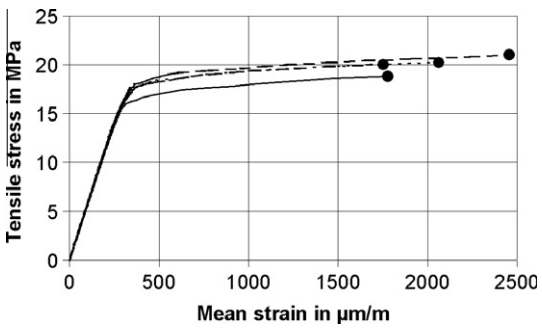

Fig. 4. Stress–strain curves related to the four specimens tested in uniaxial tension.

Fig. 5. Example of crack patterns obtained at the end of the tensile test.

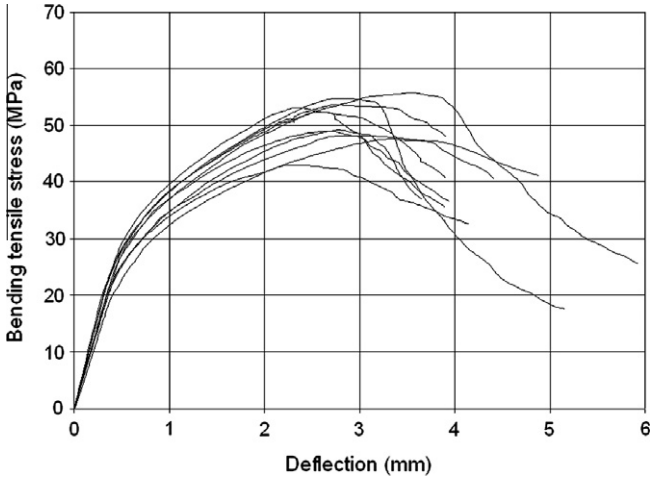

Fig. 6. Equivalent tensile stress vs. deflection curves in bending.

loading, but no experimental information is actually available to confirm this fact. Nevertheless, the choice of an elastic–plastic approach remains classical, especially in case of reinforced concrete structures.

The selected model, established in thermodynamics framework of elastic–plasticity theory, is based on the Willam and Warnke criterion [14] and aims to represent material hardening behaviour, i.e. "displacement" of the loading surface in principal stress space. Note that a complete and detailed description of this model is given in [15]. It is implemented in the CESAR-LCPC finite element code. In this model the principal useful input parameters are:

- E: the material Young's modulus,
- ν: the material Poisson ratio,
- σ_c: the material compressive strength,
- σ_t: the material tensile strength,
- ε_{tc}: the critical tensile strain,
- ξ_0, ξ_f, and κ are parameters defining the hardening of the material.

In this elasto-plastic approach adopted, the calculation is stopped when the tensile strain reaches ε_{tc}.

The logical way to use this model in the frame of this study should be:

- first, to determine the values of the input parameters (see above) by fitting the uniaxial tensile test result,
- then, to simulate the bending test with these input parameters values.

But, that is not the approach chosen in this study. As a matter of fact, it is assumed that, in reality, the material tested in the frame of the uniaxial tensile test is different from the one tested in the frame of the bending test, even though the mix design is the same. This difference can be explained by the existence of two effects:

- the preferential orientation of the longest fibres at the bottom of the mould ("wall effect");
- the logical segregation of the same longest fibres (which are also the heavier) always at the bottom of the mould.

This non-uniform distribution and orientation of fibres in specimens respectively loaded in uniaxial tension and in bending is illustrated in Fig. 7.

In the frame of the "multi-scale fibre reinforcement" concept [1] the longest fibres (low percentage) are responsible for the material ductility and the smaller ones (high percentage) are responsible for the strength. Moreover, the existence of a non-uniform orientation of fibres related to the specimen stress distribution exists in both tests (Fig. 7). This could induce some difference of ductility (some difference in the value of ε_{tc}) given by the two types of tensile test (direct and indirect).

In order to verify the pertinence of this assumption, a semi-inverse approach has been chosen which can be summarised as the following:

- First, the tensile test is fitted to determine the parameters σ_t, ε_{tc}, ξ_0, ξ_f and κ of the model. The values of the others parameters like E, ν, σ_c, come from a previous study [4].
- Secondly, the bending tests are fitted with the hardening parameters values obtained from the first step (the assumption that the hardening behaviour mechanisms of the material are the same in uniaxial tension and in bending). So, only σ_t has to be chosen for the fitting. The calculation is stopped for a deflection corresponding to the experimental modulus of rupture. The calculated value of ε_{tc} (at the lower face of the bending specimen) is then determined.

6. Numerical results

Numerical simulations of tensile and bending tests are performed, using a plain stress computation. Fig. 8 presents the fitting of the tensile test and the corresponding parameters values. Fig. 9 presents the fitting of the bending test.

In this latter figure the term "stress" denotes equivalent tensile stress at the lower level of median cross section of specimen. Its expression is given by extrapolation of classical formula of the strength of materials theory in the nonlinear domain of the mechanical material behaviour:

$$\sigma = \frac{M_f}{I/V} = \left(\frac{bh^2}{6} l_e\right) \times F \tag{1}$$

h and b are dimensions of the cross section. l_e represents the distance between the support and the load application point. Thus, in this sense, this stress can be representative of applied load F.

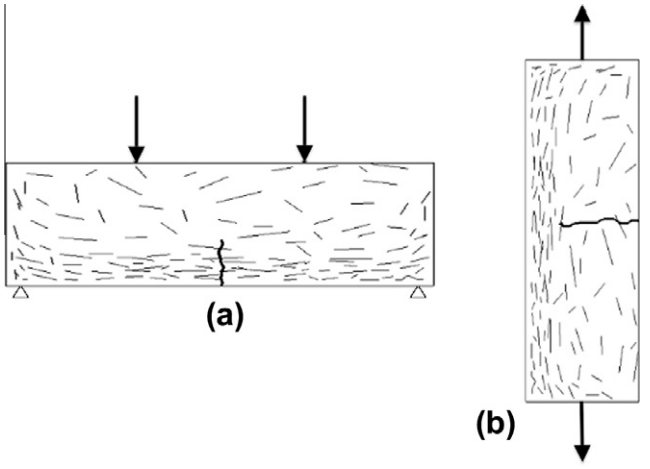

Fig. 7. Effects of the fibres orientation on the crack localisation (a) under a 4-point bending test and (b) under an uniaxial tensile test.

The fitted numerical curve is obtained for a uniaxial tensile strength of 21 MPa. The computed axial strain at the lower face of the specimen is 5.1×10^{-3}. The first remark concerns the fact that the computed results related to uniaxial tensile strength and to axial strains at lower face of specimen are in very good accordance with the experimental results (around 20 MPa given by the uniaxial tensile test, and 5×10^{-3} given by the bending test). The second remark concerns the fact that the computed value of the critical tensile strain (5.1×10^{-3}) is twice the experimental one (2.5×10^{-3}). This point confirms the assumption that the tensile behaviour of the studied material is more ductile in bending than in uniaxial tension.

7. Study of an eventual scale effect in bending

7.1. Experimental part

The objective of this part is to study the possible scale effect related to the bending behaviour of the studied MSCC. To achieve this objective, another specimen geometry has been chosen to be tested in bending. It is a small beam: 400 mm length, 100 mm width and 100 mm thickness. This beam is also submitted to a 4-point bending test.

The distance between the lower supports is 300 mm; the distance between the higher supports is 100 mm. Tests are carried out at an imposed deflection rate equal to 0.3 mm/min. Deflection is measured using the same device than for the above tests on the plate-like specimens. Nine specimens are tested.

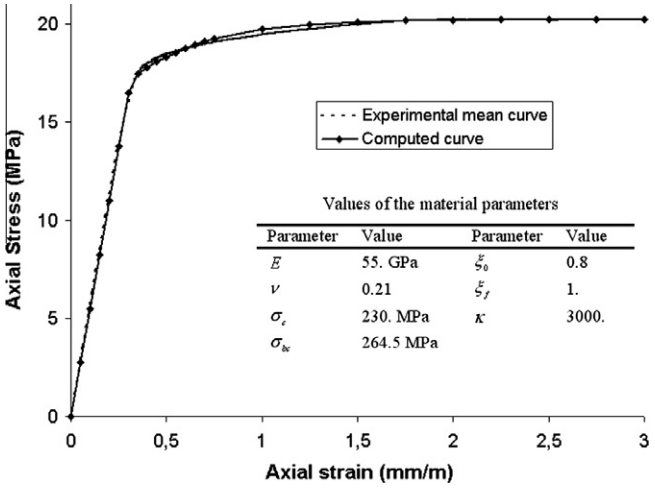

Fig. 8. Simulation of the tensile test and comparison with the experimental result (mean curve – axial stress vs. axial strain).

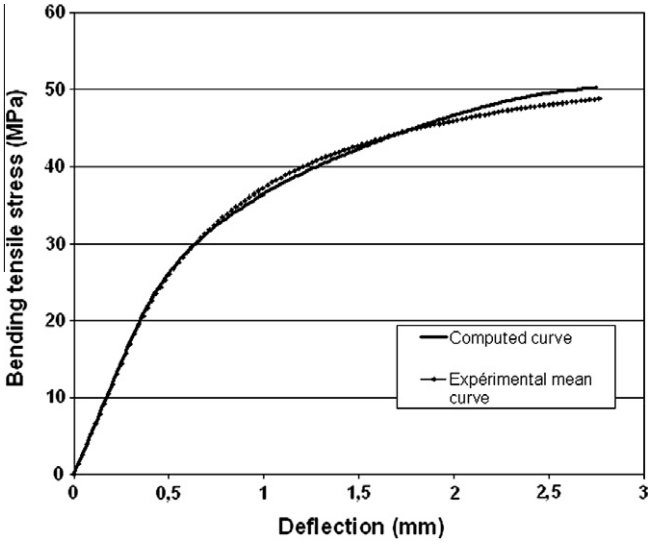

Fig. 9. Simulations of the bending test and comparison with the experimental result (mean curve – equivalent tensile stress vs. deflection).

7.2. Numerical modelling

To study a possible scale effect related to the bending behaviour of the studied material, it has been chosen to use the values of the model parameters (described above) obtained from the numerical analysis of the 4-point bending test on the small plates to simulate the 4-point bending behaviour of these small beams.

7.3. Comparisons between numerical simulations and experimental results

Fig. 10 presents the comparison between the numerical simulation and the experimental result related to bending tests on the small beam. A look of this figure leads to the following conclusion: the comparison between the numerical simulation and the experimental results is very good. And the following remarks can be drawn:

- firstly, the chosen model and the determined material parameters are physically pertinent in the frame of the structural behaviour and the specimen geometries;
- secondly, structural elements made of the studied material do not seem to have a bending capacity sensitive to a significant scale effect. This conclusion is relevant for the domain of the structural applications aimed with this material;
- finally, the studied material can be considered as having an elasto-plastic behaviour with strain hardening in tension if we consider its use in structures (whose the thickness is no more than 100 mm) subjected to bending. This last remark is, of course, linked to the first one.

8. Conclusions

The development of a new uniaxial tensile test to study a strain hardening cement composite is presented in this paper. The specimen geometry and the test-set up have been optimised to obtain homogeneous stress and strain fields in the specimen central part,

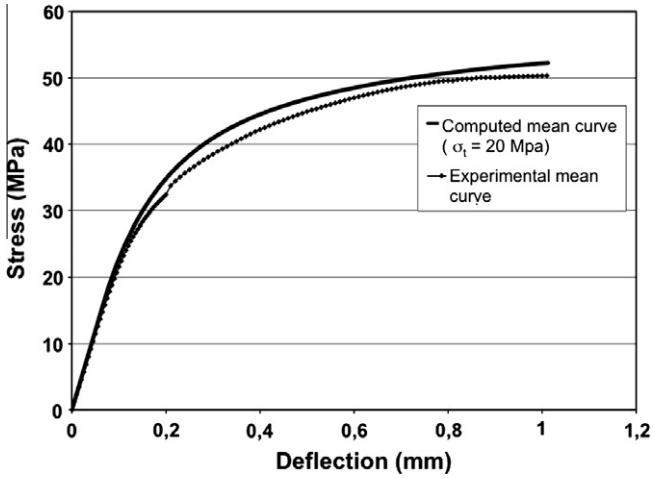

Fig. 10. Comparison of numerical simulation/experiments related to bending behaviour of the small beam.

where the strain measurement is performed. The experimental results, obtained with this tensile test, show that there is no bending of the specimen until the peak load. This condition is very important and difficult to obtain to demonstrate that the studied material is really a strain hardening one.

This paper shows that the use of a "classical" elasto-plastic behaviour with strain hardening is pertinent to the design of structural elements made with the studied material.

A semi-inverse approach allows to determine the values of the model parameters to be taken into account in the finite element simulations. Finally, it is shown that these parameter values are not sensitive to scale effects for designing structural elements whose thickness does not exceed 10 cm.

References

[1] Rossi P, Acker P, Malier Y. Effect of steel fibres at two stages: the material and the structure. Mater Struct 1987;20:436–9.
[2] Rossi P. High performance multimodal fibre reinforced cement composite (HPMFRCC): the LCPC experience. ACI Mater J 1997;94(6):478–83.
[3] Parant E. Mécanismes d'endommagement et comportements mécaniques d'un composite cimentaire fibré multi-échelles sous sollicitations sévères: fatigue, choc, corrosion. Etudes et Recherches des Laboratoires des Ponts et Chaussées, no. OA45; 2004 [in French].
[4] Rossi P, Arca A, Parant E, Fakhri P. Bending and compressive behaviours of a new cement composite. Cem Concr Res 2005;35:27–33.
[5] Parant E, Rossi P, Boulay C. Fatigue behaviour of a multi-scale fibre reinforced cement composite. Cem Concr Res 2007;37:264–9.
[6] Parant E, Rossi P, Le Maou F. Durability of a multi scale fibre reinforced cement composite in aggressive environment under service load. Cem Concr Res 2007;37:1106–14.
[7] Parant E, Rossi P, Jacquelin E, Boulay C. Strain rate effect on the bending behaviour of new ultra-high performance cement composite. ACI Mater J 2007;104:458–63.
[8] Rossi P, Parant E. Damage mechanisms analysis of a multi-scale fibre reinforced cement-based composite subjected to impact and fatigue loading conditions. Cem Concr Res 2008;38:413–21.
[9] Denarié E, Brühwiler E. Tailored composite UHPFRC-concrete structures. In: Konsta-Gdoutos MS, editor. Proceedings measuring, monitoring, and modelling concrete properties. Proceedings MMCP symposium. Springer; 2006. p. 69–75.
[10] Benson SDP, Karihaloo BL. CARDIFRC – development and mechanical properties. Part III: Uniaxial tensile response and other mechanical properties. Mag Concr Res 2005;57(8):433–43.
[11] Do MT. Fatigue des BHP. PhD thesis. Sherbrooke, Sherbrooke University; 1994 [in French].
[12] Behloul M. Définition d'une loi de comportement du BPR. Ann de l'ITBTP 1995;532:122–7 [in French].
[13] Behloul M. Analyse et modélisation du comportement d'un matériau à matrice cimentaire fibrée à ultra hautes performances – (béton de poudres réactives) – Du matériau à la structure. PhD thesis. Cachan, Ecole Normale Supérieure de Cachan; 1996 [in French].
[14] Willam KJ, Warnke EP. Constitutive model for the triaxial behaviour of concrete. Int Assoc Bridge Struct Eng. Seminar on concrete structures. Paper III-1, IABSE proc 19, Bergamo, Italy; 1975.
[15] Ulm FJ. Un modèle d'endommagement plastique: application aux bétons de structure. Etudes et Recherches des Laboratoires des Ponts et Chaussées, no. OA19; 1996 [in French].